Magnetic structure and metamagnetism in single crystals of $NpCoGa_5$

N. Metoki,[1,2,*] K. Kaneko,[1] E. Colineau,[3] P. Javorský,[3,4] D. Aoki,[5] Y. Homma,[5] P. Boulet,[3] F. Wastin,[3] Y. Shiokawa,[1,5] N. Bernhoeft,[6] E. Yamamoto,[1] Y. Ōnuki,[1,7] J. Rebizant,[3] and G. H. Lander[1,3]

[1]*Advanced Science Research Center, Japan Atomic Energy Research Institute, Tokai, Naka, Ibaraki 319-1195, Japan*

[2]*Department of Physics, Tohoku University, Sendai 980-8578, Japan*

[3]*European Commission, JRC, Institute for Transuranium Elements, Postfach 2340, D-76125 Karlsruhe, Germany*

[4]*Department of Electronic Structures, Faculty of Mathematics and Physics, Charles University, Ke Karlovu 5, 12 116, Prague 2, The Czech Republic*

[5]*Institute for Materials Research, Tohoku University, Oarai, Ibaraki 311-1313, Japan*

[6]*CEA, Département de Recherche Fondamentale sur la Matière Condensée, 38054 Grenoble Cedex 9, France*

[7]*Graduate School of Science, Osaka University, Toyonaka, Osaka 560-0043, Japan*

(Received 15 March 2005; published 25 July 2005)

The magnetic structure and *H-T* phase diagram of $NpCoGa_5$ single crystals (space group P4/mmm) have been investigated by neutron diffraction, magnetization, and specific heat. The antiferromagnetic ordering at $T_N=47$ K has a wave vector $\mathbf{q}=(0\ 0\ 1/2)$, corresponding to a simple $+-$ arrangement of the Np moments stacked along the tetragonal *c* axis, with the Np moments pointing along *c*. The Np magnetic moment 0.8(1) μ_B/Np, deduced from the present neutron experiments, is consistent with the results of the magnetization measurements 0.70(2) μ_B/Np in the high-field ferromagnetic state and previous Mössbauer studies on polycrystalline sample 0.84(5) μ_B/Np. The magnetic scattering intensity is well explained without any moment on the Co atom and the magnetic form factor is consistent with the presence of a significant orbital moment on the Np site. The susceptibility shows Curie-Weiss behavior with strong anisotropy in the antiferromagnetically ordered state. The Sommerfeld coefficient is $\sim$65 mJ mol^{-1} K^{-2} in both the antiferromagnetic and field-induced ferromagnetic states. With an applied magnetic field along the *c* axis a first-order metamagnetic transition occurs with rather low critical field [$\mu_0 H_c$ $(T=0)=4.5$ T]. No metamagnetic transition has been observed for fields up to 9 T applied perpendicularly to *c*. The small metamagnetic field compared to the high magnetic ordering temperature indicates that the ferromagnetic coupling within each ferromagnetic Np plane is strong, but the antiferromagnetic interplanar coupling is relatively weak.

DOI: 10.1103/PhysRevB.72.014460 PACS number(s): 75.30.−m, 71.27.+a, 74.10.+v, 75.25.+z

I. INTRODUCTION

Actinide-based "115" compounds $AnTGa_5$ (An=U,[1–11] Np,[12–17] Pu,[18,19] T: Transition metal elements) have attracted much attention since the discovery of a relatively high superconducting $T_c \approx 9$ K in $PuCoGa_5$,[18] followed by a $T_c \approx 18$ K in $PuRhGa_5$.[19] These materials crystallize in the tetragonal $HoCoGa_5$-type structure with the space group P4/mmm. The structure consists of a sequential stacking of $AnGa_3$ with $AuCu_3$ structure and TGa_2 crystallographic layers along the tetragonal axis, where T=Fe, Co, Ni, Ru, Rh, Pd, Os, Ir, and Pt.

Prior to the Pu-115 compounds, U-115 systems were studied.[1–11] Despite the availability of high-quality single crystals, no superconductivity has been reported at either ambient or under high pressures.[20,21] More recently, high-quality single crystals of $NpTGa_5$ (T=Fe, Co, Ni, and Rh) have been grown.[12–17] So far, no superconductivity has been reported in Np-115 compounds; rather they appear to exhibit magnetically ordered ground states.

Heavy-Fermion superconductivity in isostructural Co-, Rh-, and Ir-based compounds was first reported in $CeRhIn_5$ under pressure.[22] This was followed by discoveries of superconductivity in $CeCoIn_5$ and $CeIrIn_5$ at ambient pressure.[23–25] In these papers, the authors propose that the marked tetragonality of the unit cell enforces a quasi-two-dimensional electronic structure which enhances the superconductivity originally found[26] in the cubic compound $CeIn_3$ in the vicinity of the quantum critical point under pressure.[27] The rich variety of electronic structures with different numbers of *f* and *d* electrons in this family of rare-earth and actinide compounds should allow the development of a systematic understanding of these strongly correlated *f* electron systems.

Given the similar quasi-two-dimensional electronic structure, the existence of the superconductivity in Ce and Pu compounds and its absence in U and Np compounds has been attributed to the strongly itinerant character of 5*f* bands in the latter. This favors Pauli-paramagnetism in U-115 with itinerant magnetic states predominating in Np-115 materials.[28–31]

In this paper, the results of neutron scattering, magnetization, and specific-heat experiments on single-crystal samples of $NpCoGa_5$ are reported. This compound, which has been studied by resistivity,[13] magnetic susceptibility,[13,14] specific heat,[13,14] and Mössbauer spectroscopy measurements,[13] exhibits a modified Curie-Weiss behavior and a phase transition at 47 K. From these data, it was suggested that the transition was to a type I antiferromagnetic structure with magnetic moments of 0.84(5) μ_B/Np aligned along the *c* axis.[13] No superconductivity was observed down to $T=0.4$ K.[13] Metamagnetism was revealed by the bulk measurements on polycrystalline samples,[13] motivating the

present neutron diffraction and thermodynamic studies on $NpCoGa_5$ single crystals under an applied magnetic field.[14] In particular, neutron diffraction is important to establish the antiferromagnetic nature of the 47 K phase transition, the form factor and the ordering wave vector of the antiferromagnetic structure.

II. EXPERIMENT

The great difficulty of transporting materials containing transuranium nuclides has meant that the single-crystal samples used for these measurements were grown in two different institutions. Those used in thermodynamic measurements were grown at the Institute for Transuranium Elements (ITU), Karlsruhe, and those used for the neutron diffraction experiments were grown at the Oarai facility of the Institute for Materials Research, Tohoku University.[14] In both cases, the methods were based on growth within a Ga flux.[32] While this duplication in sample preparation is a major undertaking, it does yield important consistency checks that guarantee a more robust final result.

Neutron scattering experiments have been carried out on the cold and thermal triple-axis spectrometers LTAS and TAS-2, respectively, installed at the research reactor JRR-3 in Japan Atomic Energy Research Institute (JAERI), Tokai. The neutron beam was monochromatized and analyzed via vertically bent pyrolytic graphite (PG) crystals with the collimation of 26′-80′-80′-80′ at incident energy $E=4.9$ meV and 15′-80′-40′-80′ at $E=30.5$ meV for LTAS and TAS-2, respectively. Harmonic contamination of the incident beam was removed by a cooled Be filter at 20 K and a PG filter for the cold and thermal neutron experiments, respectively. The sample of dimensions $3\times3\times1$ mm^3 was mounted on a sample holder with the [1 1 0] and [0 0 1] axes in the horizontal scattering plane, and sealed in an aluminium sample cell filled with He exchange gas. The sample cell was cooled in a closed cycle refrigerator down to 3 K or in a cryomagnet down to 1.5 K, with the horizontal field applied ($H_{max}=5$ T) along the c axis.

Macroscopic measurements were performed at ITU. dc-magnetization measurements of $NpCoGa_5$ were performed on a commercial *Quantum Design* superconducting quantum interference device magnetometer from 2 K to 300 K in magnetic fields up to 7 T. The specific heat was measured on a commercial *Quantum Design Physical Property Measurement System* (PPMS) instrument by the relaxation method within the temperature range of 1.8–300 K in magnetic fields up to 9 T.

III. RESULTS

The results of the neutron-diffraction experiments in zero field to determine the magnetic structure (Fig. 1), the magnitude of the moment, and the magnetic form factor will be presented first; followed by the results of all techniques with the application of a magnetic field.

A. $H=0$

Figure 2 shows representative neutron diffraction data along the (1 1 l) for $-1.6<l<1.6$ reciprocal lattice units.

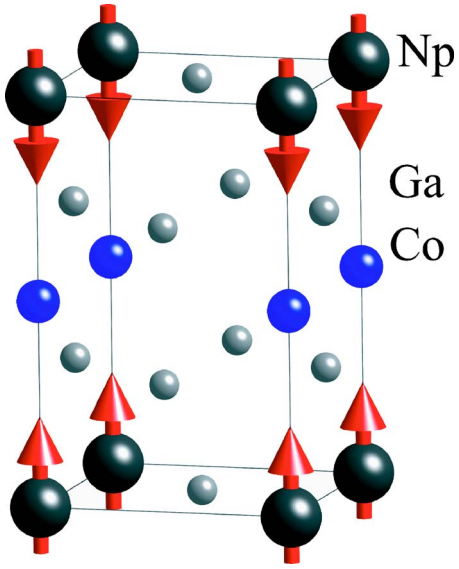

FIG. 1. (Color online) The crystal and magnetic structure of $NpCoGa_5$ shown in the crystallographic unit cell. The large dark gray circles with the red arrows to represent the magnetic moments are the Np atoms, the Co atoms illustrated by medium blue (black) balls are at the middle crystallographic layer of the unit cell, and there are two sets of Ga atoms (smallest gray spheres).

Superlattice peaks at (1 1 ±0.5) and (1 1 ±1.5) were observed at $T=3.5$ K in addition to the strong (1 1 0) and (1 1 ±1) nuclear reflections. The superlattice peaks, which are absent above the magnetic transition $T_N=47$ K are attributed to an antiferromagnetic structure with a magnetic propagation vector $\mathbf{q}=(0\ 0\ 1/2)$. Searches were made along the (0 0 l) (h h 0), and (h h l) scattering directions, but no additional superlattice peak was observed. The magnetic structure can be described by a simple repeat along the c axis with

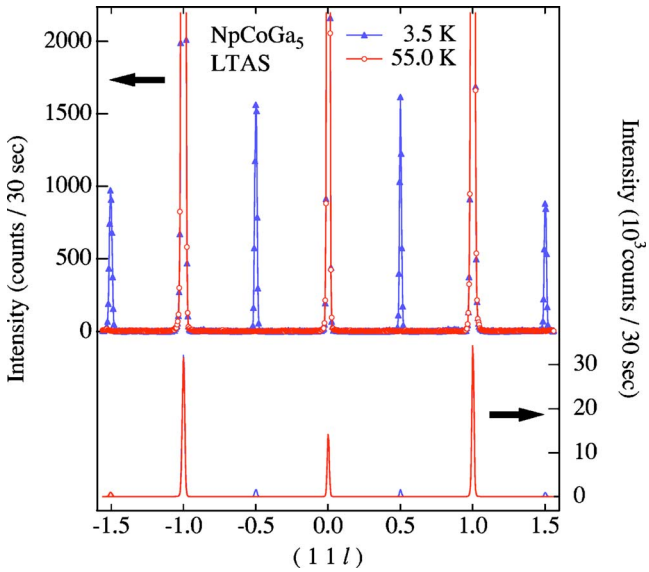

FIG. 2. (Color online) Upper panel gives the (1 1 l) neutron scattering profile of $NpCoGa_5$ at $T=3.5$ K below T_N and $T=55$ K above T_N, denoted by closed triangles and open circles, respectively. Lower panel gives the same data on a reduced scale.

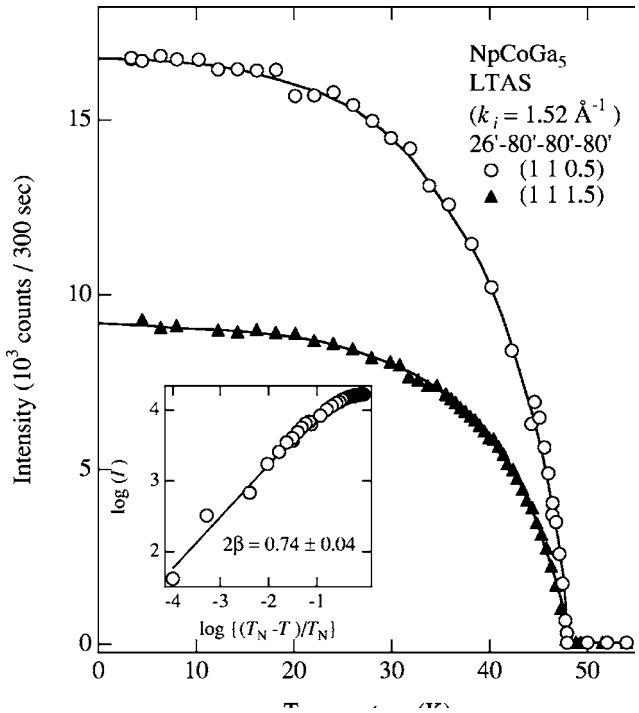

FIG. 3. The temperature dependence of the (1 1 0.5) and (1.1 1.5) antiferromagnetic peak intensity, denoted by open circles and closed triangles, respectively. The lines are a guide for the eyes. The inset is a logarithmic plot of the (1 1 0.5) intensity data. The solid line represents the curve with the critical exponent of the magnetic order parameter $2\beta=0.74$ (4), and $T_N=47.9$ K.

alternate ferromagnetic planes of Np moments coupled antiferromagnetically as shown in Fig. 1. The absence of the magnetic reflections along the (0 0 l) direction implies that the moment is along this axis. This confirms the Mössbauer result[13] that the hyperfine field is parallel to the quantization c axis; the same magnetic structure is found in $UPtGa_5$ and $UPdGa_5$.[9,33]

The (1 1 0.5) and (1.1 1.5) antiferromagnetic peak intensities were measured as a function of temperature as shown in Fig. 3 giving $T_N=47.9$ K. The inset shows the (1 1 0.5) intensity with logarithmic scales. Whilst the estimated exponent of the magnetic order parameter $\beta=0.37(2)$ is somewhat higher than the value for a three-dimensional Ising system $\beta=0.33$, and closer to that of the three-dimensional (3D) Heisenberg value of 0.367, in the latter case it would be unusual to have directional anisotropy in the field dependence of the antiferromagnetic structure, see below.

Figure 4 summarizes the integrated intensity of the antiferromagnetic reflections in the (h h l) scattering plane. The magnetic scattering intensity for unpolarized neutron diffraction experiments can be written as

$$I_{\mathrm{mag}}(\mathbf{Q}) \propto |F_{\mathrm{mag}}(\mathbf{Q})|^2 \mu^2 f^2(\mathbf{Q})(\sin\alpha)^2 L(\theta), \qquad (1)$$

where F_{mag} is the magnetic structure factor, $f(\mathbf{Q})$ is the magnetic form factor, α is the angle between the ordered magnetic moment and the scattering vector $\mathbf{Q}$, and $L(\theta)$ is the Lorentz factor. In the model calculation, the simple collinear antiferromagnetic structure shown in Fig. 1 was assumed

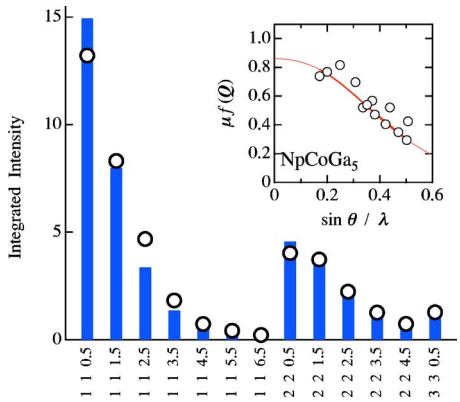

FIG. 4. (Color online) Antiferromagnetic reflection intensities of $NpCoGa_5$. Open circles represent the experimental results and the bars denote the calculated ones assuming the magnetic structure shown in Fig. 1 together with the Np^{3+} form factor. The inset gives the experimental (circles) and fitted Np^{3+} (line) form factor using $C_2=2.33$. The antiferromagnet ordered moment of neptunium is deduced to be 0.8(1) μ_B/Np.

without any moment on the Co site, i.e. the magnetic moment is associated only with the Np ion. It is notable also that, in the magnetic structure, the exchange field from Np moment on the Co site is canceled.

The magnetic structure factor F_{mag} is unity for all reflections for this antiferromagnetic structure. As Mössbauer experiments indicate a Np^{3+} charge state,[13] the magnetic form factor for Np^{3+} free ion was used.[34] As shown in Fig. 4, the experimentally observed intensity denoted by open circles can be well reproduced by the model calculation presented by solid bars. The magnetic moment of Np is 0.8(1) μ_B/Np, in good agreement with a value of 0.84(5) μ_B obtained by Mössbauer spectroscopy.[13]

B. $H>0$

The induced ferromagnetic moment exhibits a field and temperature dependent transition with the magnetic field applied along the c axis as shown in Fig. 5. The response measured in 7 T approaches saturation at a value of 0.70(2) μ_B/Np at 5 K.

When the magnetic field is applied perpendicular to the c axis, no such metamagnetic transition was observed (inset Fig. 5). In this direction, the paramagnetic to antiferromagnetic transition as monitored through the susceptibility appears to be unaffected by fields up to $\mu_0 H=7$ T. The absence of a metamagnetic-like transition for fields in this range applied in the basal plane is confirmed by $M(H)$ curves as shown in Fig. 6 at $T=5$ K.

In the paramagnetic state, the magnetic susceptibility can be described by a modified Curie-Weiss law (Fig. 7). The parameters, derived from the M/H ratio at 1 Tesla, take different values when measured with the field applied along or perpendicular to the c axis. The effective moments are $\mu_{\mathrm{eff}}=1.65$ μ_B and 1.40 μ_B, the paramagnetic Curie temperatures $\theta_p=40$ K and 1.4 K and the constant terms $\chi_0=2.70\times10^{-4}$ emu/mol and 2.03×10^{-4} emu/mol,

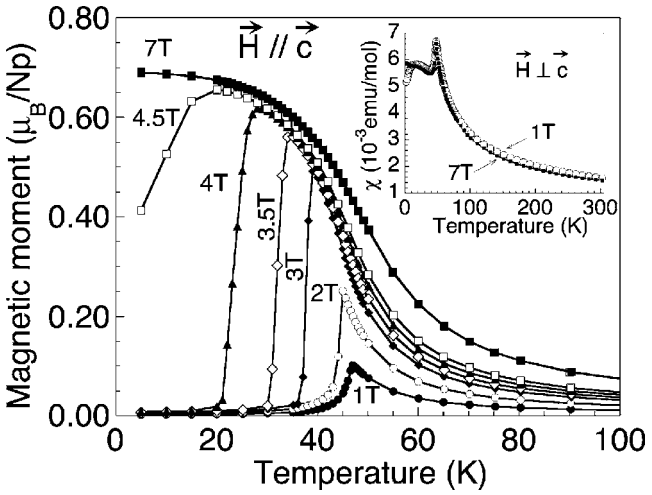

FIG. 5. Magnetic moment per Np ion of a $NpCoGa_5$ single crystal for different applied magnetic fields, along the c axis. The inset shows the magnetic susceptibility with $\mathbf{H} \perp c$.

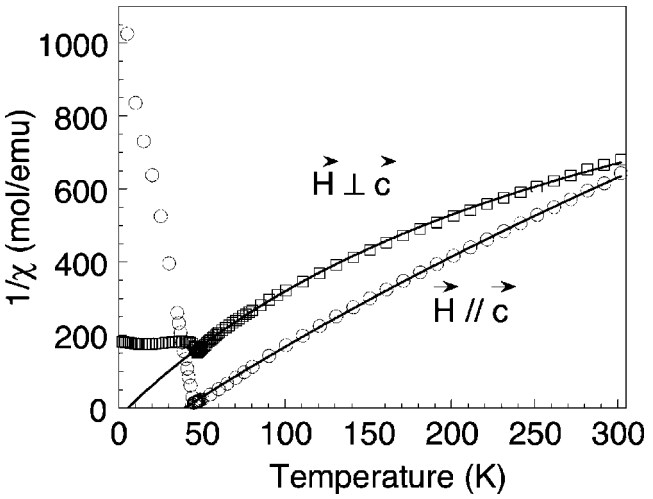

FIG. 7. Inverse magnetic susceptibility of $NpCoGa_5$ measured with $\mathbf{H} \perp c$ (squares) and $\mathbf{H} \| c$ (circles) taken with a $\mu_0 H = 1$ T. The solid lines represent the modified Curie–Weiss fits to the data.

respectively. The large difference in θ_p for the different field directions is attributed to a strong uniaxial anisotropy. The effective moment compares well with the averaged value from the polycrystalline sample: $\mu_{\text{eff}} = 1.50\ \mu_B$.[13]

The shift of the transition temperature is also clearly observed by specific heat measurements for $\mathbf{H} \| c$, as shown in Fig. 8. Additional information provided by Fig. 8 is the evolution of the peak accounting for the antiferromagnetic ordering from a lambda shape, indicating a second-order transition, to a narrow intense peak, revealing a first-order transition. From the inset of Fig. 8, it is clear that the antiferromagnetic-to-ferromagnetic transition observed by increasing the magnetic field, e.g., at $T = 40$ K is also first order. The implications for the magnetic phase diagram are developed in the discussion. Figure 9 details, on an expanded scale, the change in form with $\mathbf{H} \| c$. For $H = 0$, we observe a clear lambda-type anomaly typical of a second-order transition with weak fluctuations above T_N. On cooling, at $\mu_0 H = 3$ T, a broad anomaly in the range $37\ \text{K} < T < 47$ K is attributed to a crossover from the paramagnetic to a field-induced ferromagnetic state. The sharp C/T peak at 37 K is related to a first-order transition from induced ferromagnetism to antiferromagnetism. At the highest experimental field, $\mu_0 H = 9$ T, the anomaly related to the crossover from the paramagnetic state to the field-induced ferromagnetic state shows a broadening, indicative of the presence of ferromagnetic fluctuations up to ~70 K. The antiferromagnetic phase is completely suppressed for fields above 4.5 T, even at the lowest accessible temperatures.

For $\mathbf{H} \perp c$, as monitored through the susceptibility (Fig. 5), the effect of a 7 T magnetic field is apparently small. However, for a field of 3 T there is already a significant shift, of about 4 K, with concomitant sharpening in the phase transition anomaly as revealed by the specific heat (Fig. 10). The magnitude of shift and peak height of the C/T transition anomaly are similar to those occurring for $\mathbf{H} \| c$ and almost certainly represent a reduction in T_N as there is no evidence in the magnetization of a ferromagnetic transition with $\mathbf{H} \perp c$.

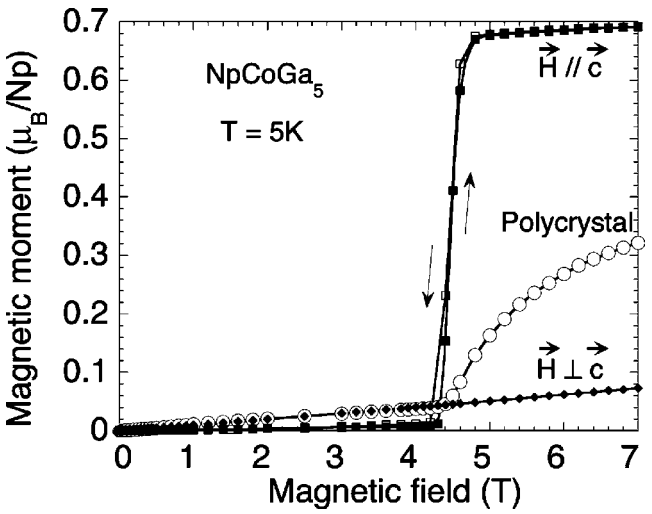

FIG. 6. Magnetic moment per Np ion of a $NpCoGa_5$ single crystal at $T = 5$ K with $\mathbf{H} \| c$ and $\mathbf{H} \perp c$. The magnetic moment per Np ion of the polycrystalline sample[13] is also shown, for comparison.

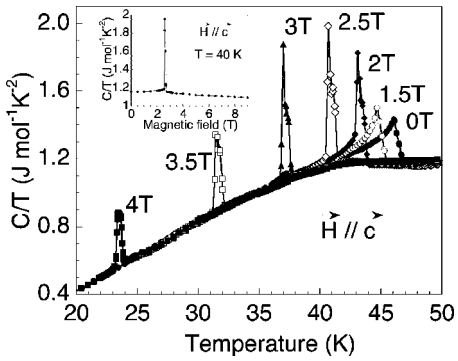

FIG. 8. C/T ratio of $NpCoGa_5$ measured with different values of the magnetic field oriented along the c axis. The inset gives C/T at $T = 40$ K as a function of the magnetic field.

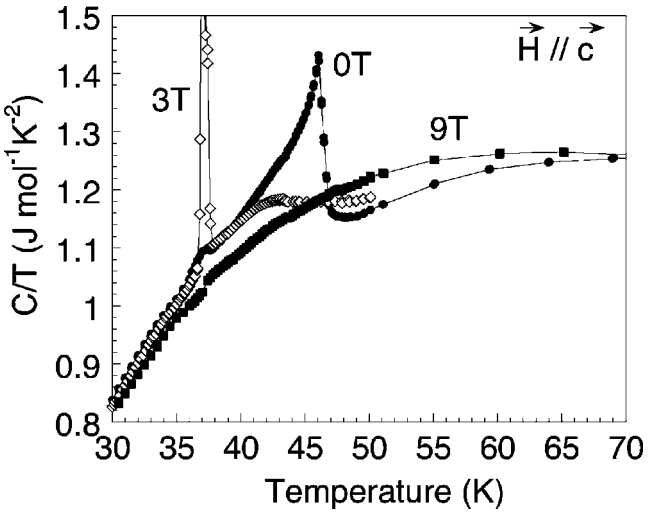

FIG. 9. C/T ratio of $NpCoGa_5$ under magnetic field along the c axis on an expanded scale. The change in form at three characteristic fields from a λ-like second-order transition at 0 T, to a broad crossover plus spike at 3 T and finally a smeared crossover at 9 T is evident.

Neutron diffraction experiments under magnetic fields for $\mathbf{H}\|c$ have been carried out to clarify the magnetic structure at 4.6 T, i.e. above the low-temperature metamagnetic transition field. As shown in Fig. 11, the (1 1–1.5) antiferromagnetic reflection peak observed for $H=0$ at $T=1.6$ K disappears. Although, for technical reasons, we could not scan in wide $\mathbf{Q}$ range to confirm the absence of any supperlattice peak with different position from $\mathbf{q}=(0\ 0\ 1/2)$, we believe that, from the agreement between the high-field ferromagnetic moment measured by the magnetization and antiferromagnetic moment determined for $H=0$, a simple ferromagnetic structure with moment parallel to the c axis appears for high field.

Figure 12 demonstrates the field dependence of the (1 1 1.5) antiferromagnetic peak height measured for various

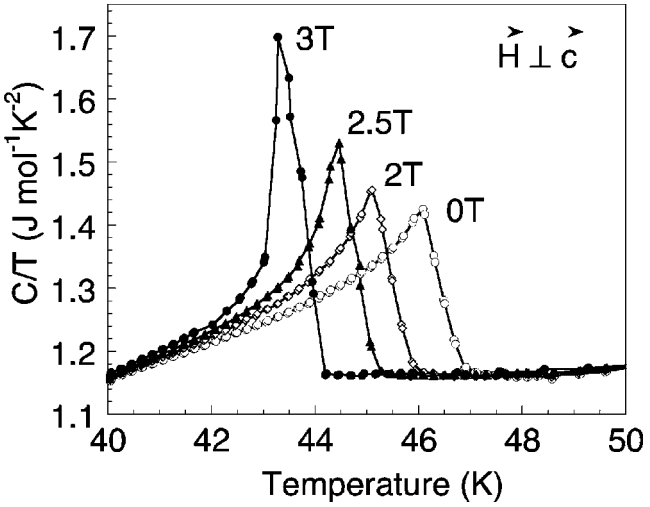

FIG. 10. C/T ratio denoting the shift in Néel temperature of $NpCoGa_5$ measured with different values of the magnetic field oriented perpendicular to the c axis.

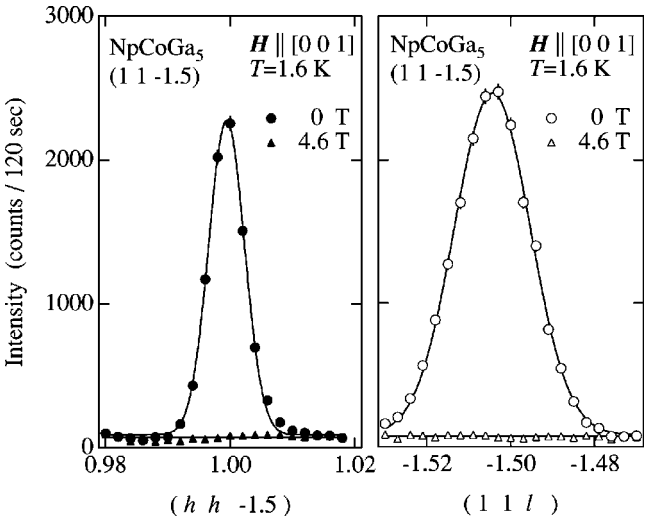

FIG. 11. The (1 1 1.5) antiferromagnetic reflection of $NpCoGa_5$ measured without magnetic fields (open and closed circles). The peak disappears with application of the magnetic field $\mu_0 H=4.6$ T along the c axis as shown by open and closed triangles. The left- and the right-hand side panels are scans along the (h h 0) and the (0 0 l) directions, respectively.

temperatures below T_N. The antiferromagnetic intensity has a weak field dependence below $H_c(T)$ for $T<40$ K and drops to the background level for $H \geqslant H_c(T)$, confirming the first-order transition revealed by specific-heat measurements. When the temperature is close to the antiferromagnetic ordering temperature, $T_N=47$ K, the antiferromagnetic intensity decreases more gradually to the background level, with increasing H. This is in agreement with the specific heat showing that the magnetic transition in the vicinity of T_N is second-order (see inset to Fig. 8 and phase diagram discussion below).

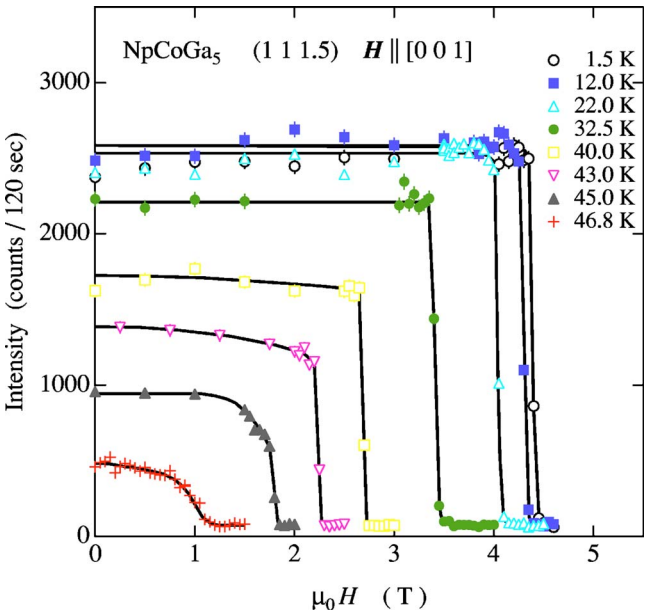

FIG. 12. (Color online) The field dependence of the (1 1 1.5) antiferromagnetic peak intensity of $NpCoGa_5$ measured at various temperatures. The field is applied parallel to the c axis.

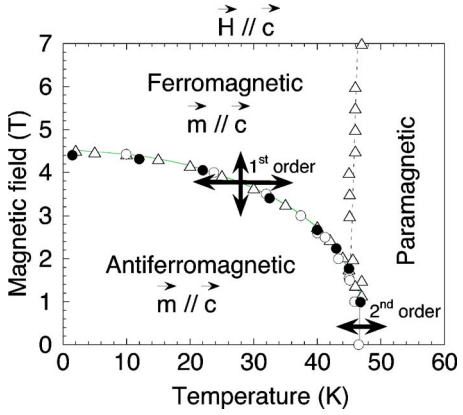

FIG. 13. (Color online) The *H-T* magnetic phase diagram of $NpCoGa_5$. The symbols represent the phase boundaries for a crystal oriented with the *c* axis along **H**, inferred from magnetization (triangles), specific heat (open circles) and neutron diffraction (full circles). The solid lines are a guide for the eyes and the dashed line represents the crossover from paramagnetism to induced ferromagnetism. The intersection of these two lines defines the tricritical point where the metamagnetic transition character changes from first to second order. The arrows represent the magnetic transitions when increasing or decreasing the temperature (horizontal arrows) or the magnetic field (vertical arrows).

The field and temperature dependencies of the metamagnetic transition obtained by neutron scattering (the middle point of the jump), magnetization (middle point of the jump) and the specific heat anomaly (middle point of the jump for second-order transitions and peak position for first-order transitions) are plotted as a *H-T* phase diagram in Fig. 13. The phase boundaries, determined by different experimental techniques with different samples, are in excellent agreement. The paramagnetic-to-antiferromagnetic transition is second-order, this terminates at a tricritical point where the paramagnetic to induced-ferromagnetic crossover occurs and the antiferromagnetic to field-induced ferromagnetic states are separated by a first-order metamagnetic transition. To date, we have no clear, neutron diffraction, evidence for a change of antiferromagnetic phase and a splitting to a critical plus bicritical endpoint duo in the vicinity of T_N as might be anticipated within certain mean field theories of dynamical magnetic states.[35]

The structural similarity between $NpCoGa_5$ and the parent $AnGa_3$ (with the cubic $AuCu_3$ structure) has been mentioned in the introduction. A strong analogy can also be drawn between the magnetic phase diagrams of $NpCoGa_5$ and $NpGa_3$ (Ref. 36) that both show antiferromagnetism and ferromagnetism phases separated by a first-order transition. The difference is that at low temperatures in $NpGa_3$ the ferromagnetic phase is present even in zero field. This illustrates the competition between ferromagnetic and antiferromagnetic interactions that takes place in these systems.

IV. DISCUSSION

The magnetic structure of $NpCoGa_5$ is established by the present neutron scattering study. The Np magnetic moments are along the tetragonal *c* axis and order ferromagnetically in the basal plane. These ferromagnetic sheets stack antiferromagnetically along the *c* axis. This magnetic structure is the same as in $UPdGa_5$ and $UPtGa_5$ but different from that found for the $UNiGa_5$ compound.[9,33,37] The similarities and differences may be traced through the susceptibility to the Fermi surface topology.

Systematic de Haas–van Alphen studies on 115 materials[6–10,38] indicate that the compounds can be categorized either as compensated semimetal or metallic depending on the total valence electron number. Compositions with an even valence electron count are compensated metals displaying equal volumes of small hole and electron pockets in their Fermi surface, while the systems with odd valence electrons are metallic with quasi-two-dimensional large Fermi surface sheets running parallel to the *c* axis.

A set of band-structure calculations using the spin polarized fully relativistic local spin density approximation (LSDA) theory[30] obtained a ground-state magnetic structure with $\mathbf{q}=(1/2\ 1/2\ 0)$, in disagreement with experiment. Recently, the phase diagram of 115 systems was studied based on a *j-j* magnetic and orbital coupling scheme.[39] A crossover from the $\mathbf{q}=(1/2\ 1/2\ 1/2)$ to $(0\ 0\ 1/2)$ structure was inferred as a function of the relative energy splitting between two Γ_8 doublets and hopping probability of *f* electrons along the *c* axis.[39] However, no experimental evidence for an orbital effect has been found in 115 compounds.

The present study provides an experimental survey, by both microscopic and thermodynamic measurements, of the antiferromagnetic to the field-induced ferromagnetic state of $NpCoGa_5$ for $\mathbf{H}\|c$. The small critical field $\mu_0 H_c(T=0)=4.5$ T (Fig. 13) reflects a strong anisotropic interaction due to the quasi-two-dimensional Fermi surface topology of this compound. Since the ferromagnetic ordering in the basal plane does not change before and after the metamagnetic transition between the antiferromagnetic and ferromagnetic states, only the weak antiferromagnetic out-of-plane coupling is broken. Simple reasoning suggests that the critical field should therefore be similar in magnitude to the effective exchange field for the weak *c*-axis antiferromagnetic interaction. The corresponding Zeeman energy of ~ 2.4 K is one order of magnitude smaller than $T_N=47$ K suggesting, in turn, a dominant role of the in-plane ferromagnetic interaction. This is consistent with the large positive value of the paramagnetic Curie temperature along the *c* axis despite the antiferromagnetic ordering.

In the work on $UTGa_5$, the form factor showed evidence for a strong orbital component.[37] Although in the present examination of $NpCoGa_5$ the form factor has not been measured with great precision (the crystals are so perfect that they exhibit considerable extinction, thus making this task difficult), the agreement shown in Fig. 4 is sufficient to state that the orbital moment dominates and that the orbital and spin moments must be antiparallel. This is consistent with all previous neutron experiments on Np compounds and must be a major constraint on theories describing these systems. In certain cases, quenching of the orbital moment can occur, and then the moment is reduced and the form factor takes on a different shape to that used here.[40–43] There is neither evidence of such effects in $NpCoGa_5$, nor would they be

expected with a moment as large as 0.8 μ_B. Assuming an Np^{3+} form factor, with an intermediate g value of 0.643 (Ref. 34), the orbital moment would be +1.9(2) μ_B with the spin moment oppositely directed with magnitude −1.1(2) μ_B. Note that due to the lack of precision on the form factor, because of the possibility of the phenomenon of extinction affecting the measured intensities, the individual error bars on the orbital and spin moments are larger than that on the total moment itself.

A degree of delocalization of the 5f electrons in $NpCoGa_5$ was reported by a recent de Haas-van Alphen study and band-structure calculations.[28–30] The observed[15] cylindrical Fermi surface was modeled on the assumption of itinerant 5f electrons having a 5f count at the Np site close to four electrons, corresponding with a formal valence Np^{3+}. Calculation by Opahle and collaborators[30] showed that the energy minimization for $T=0$ K yields an ordered magnetic state with lattice parameters in good agreement with experiment. While Opahle *et al.*[30] and Yamagami[44] find an ordered moment close to experiment, the agreement is certainly fortuitous as the calculated spin and orbital moments on the Np site are incompatible with the experimental form factor. A more complete orbital-polarization calculation certainly needs to be done as recognized by the authors themselves.

On the other hand, Aoki *et al.*[14] have used a localized model of $5f^3$ to explain the anisotropy in the magnetization results, assuming a doublet ground state within the $\mathbf{J}=4$ manifold in the tetragonal crystal field. Their crystalline field model explains the magnetic anisotropy and the magnetic entropy of $R \ln 2$ because of the doublet ground state, but yields a magnetic moment of 1.28 μ_B which is larger than the measured value of 0.8 μ_B. Using an intermediate coupling g-factor of 0.643 instead of a Landé g-factor of 0.6, would lead to an even larger moment of 1.3 μ_B. The reduced moment determined experimentally, smaller than the localized model, might reasonably result from the itinerant character of the 5f electrons and be compatible with the moderate electronic heat capacity enhancement of $NpCoGa_5$.

The magnetization results on single crystal from ITU and Tohoku University[14] are 0.70(2) and 0.74(2) μ_B/Np, respectively. On the other hand, the Mössbauer on a polycrystalline sample gives 0.84(5) μ_B/Np. The difference of −0.12(6) μ_B/Np between the two inferred values has been the subject of much discussion and has been ascribed to the polarization of the conduction (6d7s) electrons, which are not sensed in either the neutron or Mössbauer experiments; see Ref. 34, p. 656 *et seq.* and the analysis relevant to Np compounds in Wulff *et al.*[41] Calculations by Yamagami[44] give a value of −0.09 μ_B for the 6d polarization and we plan magnetic x-ray Compton and polarized-neutron experiments in the ferromagnetic state to investigate this further.

V. SUMMARY

The understanding emerging from this combination of neutron diffraction, magnetization, and specific-heat on single crystals of $NpCoGa_5$ is the following:

(1) The compound orders with $\mathbf{q}=(0\ 0\ 1/2)$ and magnetic moments of 0.8(1) μ_B/Np oriented along the c axis of the tetragonal structure.

(2) Any moment on the Co site is below present experimental sensitivity.

(3) The Np form factor is consistent with that deduced for many Np compounds, and strongly supports the idea that there is a large orbital moment with $|\mu_L| > |\mu_S|$, where μ_L and μ_S are the orbital and spin moments, respectively.

(4) While the critical exponent of 0.37(2) as determined by neutron diffraction is closer to the 3D Heisenberg (0.37) than the 3D Ising (0.33) value, the strong anisotropy of magnetic field studies parallel and perpendicular to the c axis (see Figs. 6, 7, and 11) suggest the Ising model to be the more appropriate one.

(5) The critical field is low for an actinide compound, that the axial antiferromagnetic coupling between the ferromagnetic sheets is weak, compared with the basal plane ferromagnetic coupling.

(6) The specific heat shows that the paramagnetic-to-antiferromagnetic transition is second order whereas the ferro-to-antiferromagnetic transition is discontinous (Fig. 8). This is consistent with the abrupt changes in magnetization and neutron response observed when crossing the metamagnetic transition.

(7) The relatively large value of the Sommerfeld coefficient of 64–70 mJ mol^{-1} K^{-2} that appears in both the antiferromagnetic and ferromagnetic states suggests that the 5f electrons are close to the Fermi level, an aspect which is confirmed by all the theories advanced so far.[28–30]

In conclusion, this work has established the magnetic structure and has completed the H-T phase diagram of $NpCoGa_5$. Several different interesting theoretical approaches are in progress and predict the magnetic ground state, but none fully reproduce the experimental data and further progress is necessary. Further new neutron inelastic scattering experiments, together with x-ray Compton and with polarized neutron diffraction, are suggested to help in developing our understanding of these systems.

ACKNOWLEDGMENTS

This study was carried out in the frame of the Actinide Association Research Agreement between JAERI, ITU, and CEA. The authors acknowledge fruitful discussions with A. Nakamura, J. P. Sanchez, R. Walstedt, and H. Yasuoka. A part of this study was financially supported by a Grant-in-Aid for Scientific Research from the Japanese Ministry of Energy, Culture, Sport and Technology (No. 16740212). One of the authors (P.J.) acknowledges the European Commission for support in the frame of the Training and Mobility of Researchers programme. The high-purity Np metals required for the fabrication of the compound at ITU were made available through a loan agreement between Lawrence Livermore National Laboratory and ITU, in the frame of a collaboration involving LLNL, Los Alamos National Laboratory and the U.S. Department of Energy.

*Electronic address: metoki@kotai3.tokai.jaeri.go.jp

[1] Yu. N. Grin, P. Rogl, K. Hiebl, J. Less-Common Met. **121**, 497 (1986).
[2] S. Noguchi and K. Okuda, J. Magn. Magn. Mater. **104–107**, 57 (1992).
[3] V. Sechovský, L. Havela, G. Schaudy, G. Hilsher, N. Pillmayr, P. Rogl, and P. Fischer, J. Magn. Magn. Mater. **104–107**, 11 (1992).
[4] K. Okuda and S. Noguchi, *Physical Properties of Actinide and Rare Earth Compounds Series 8*, edited by T. Kasuya, T. Ishii, T. Komatsubara, O. Sakai, N. Môri, and T. Saso (Publ. Office, JJAP, Tokyo, 1993), p. 32.
[5] M. Schönert, S. Corsépius, E.-W. Scheidt, and G. R. Stewart, J. Alloys Compd. **224**, 108 (1995).
[6] Y. Tokiwa, Y. Haga, E. Yamamoto, D. Aoki, N. Watanabe, R. Settai, T. Inoue, K. Kindo, H. Harima, and Y. Ōnuki, J. Phys. Soc. Jpn. **70**, 1744 (2001).
[7] Y. Tokiwa, T. Maehira, S. Ikeda, Y. Haga, E. Yamamoto, A. Nakamura, Y. Ōnuki, M. Higuchi, and A. Hasegawa, J. Phys. Soc. Jpn. **70**, 2982 (2001).
[8] Y. Tokiwa, S. Ikeda, Y. Haga, T. Okubo, T. Iizuka, K. Sugiyama, A. Nakamura, and Y. Ōnuki, J. Phys. Soc. Jpn. **71**, 845 (2002).
[9] S. Ikeda, N. Metoki, Y. Haga, K. Kaneko, T. D. Matsuda, and Y. Ōnuki, J. Phys. Soc. Jpn. **72**, 2622 (2003).
[10] S. Ikeda, Y. Tokiwa, T. Okubo, Y. Haga, E. Yamamoto, Y. Inada, R. Settai, and Y. Ōnuki, J. Nucl. Sci. Technol. **3**, 206 (2002).
[11] N. O. Moreno, J. L. Sarrao, M. F. Hundley, J. D. Thompson, and Z. Fisk (unpublished).
[12] D. Aoki, E. Yamamoto, Y. Homma, Y. Shiokawa, A. Nakamura, Y. Haga, R. Settai, and Y. Ōnuki, J. Phys. Soc. Jpn. **73**, 519 (2004).
[13] E. Colineau, P. Javorský, P. Boulet, F. Wastin, J.-C. Griveau, J. Rebizant, J. P. Sanchez, and G. R. Stewart, Phys. Rev. B **69**, 184411 (2004).
[14] D. Aoki, Y. Homma, Y. Shiokawa, E. Yamamoto, A. Nakamura, Y. Haga, R. Settai, T. Takeuchi, and Y. Ōnuki, J. Phys. Soc. Jpn. **73**, 1665 (2004).
[15] D. Aoki, Y. Homma, Y. Shiokawa, E. Yamamoto, A. Nakamura, Y. Haga, R. Settai, and Y. Ōnuki, J. Phys. Soc. Jpn. **73**, 2608 (2004).
[16] E. Colineau, F. Wastin, P. Boulet, P. Javorský, J. Rebizant, and J. P. Sanchez, J. Alloys Compd. **386**, 57 (2005).
[17] E. Yamamoto, D. Aoki, Y. Homma, Y. Shiokawa, Y. Haga, A. Nakamura, and Y. Ōnuki, Physica B **359–361**, 1099 (2005).
[18] J. L. Sarrao, L. A. Morales, J. D. Thompson, B. L. Scott, G. R. Stewart, F. Wastin, J. Rebizant, P. Boulet, E. Colineau, and G. H. Lander, Nature (London) **420**, 297 (2002).
[19] F. Wastin, P. Boulet, J. Rebizant, E. Colineau, and G. H. Lander, J. Phys.: Condens. Matter **15**, S2279 (2003).
[20] M. Nakashima, Y. Tokiwa, H. Nakawaki, Y. Haga, Y. Uwatoko, R. Settai, and Y. Ōnuki, J. Nucl. Sci. Technol. **3**, 214 (2002).
[21] M. Nakashima, Y. Haga, E. Yamamoto, Y. Tokiwa, M. Hedo, Y. Uwatoko, R. Settai, and Y. Ōnuki, J. Phys.: Condens. Matter **15**, S2007 (2003).
[22] H. Hegger, C. Petrovic, E. G. Moshopoulou, M. F. Hundley, J. L. Sarrao, Z. Fisk, and J. D. Thompson, Phys. Rev. Lett. **84**, 4986 (2000).
[23] C. Petrovic, P. G. Pagliuso, M. F. Hundley, R. Movshovich, J. L. Sarrao, J. D. Thompson, Z. Fisk, and P. Monthoux, J. Phys.: Condens. Matter **13**, L337 (2001).
[24] C. Petrovic, R. Movshovich, M. Jaime, P. G. Pagliuso, M. F. Hundley, J. L. Sarrao, Z. Fisk, and J. D. Thompson, Europhys. Lett. **53**, 354 (2001).
[25] R. Movshovich, M. Jaime, J. D. Thompson, C. Petrovic, Z. Fisk, P. G. Pagliuso, and J. L. Sarrao, Phys. Rev. Lett. **86**, 5152 (2001).
[26] N. D. Mathur, F. M. Grosche, S. R. Julian, I. R. Walker, D. M. Freye, R. K. W Haselwimmer, and G. G. Lonzarich, Nature (London) **394**, 39 (1998).
[27] P. Monthoux and G. G. Lonzarich, Phys. Rev. B **59**, 14598 (1999).
[28] I. Opahle and P. M. Oppeneer, Phys. Rev. Lett. **90**, 157001 (2003).
[29] T. Maehira, T. Hotta, K. Ueda, and A. Hasegawa, Phys. Rev. Lett. **90**, 207007 (2003).
[30] I. Opahle, S. Elgazzar, K. Koepernik, and P. M. Oppeneer, Phys. Rev. B **70**, 104504 (2004).
[31] T. Maehira, T. Hotta, K. Ueda, and A. Hasegawa, cond-mat/0412647.
[32] E. G. Moshopoulou, Z. Fisk, J. L. Sarrao, and J. D. Thompson, J. Solid State Chem. **158**, 25 (2001).
[33] Y. Tokiwa, Y. Haga, N. Metoki, Y. Ishii, and Y. Ōnuki, J. Phys. Soc. Jpn. **71**, 725 (2002).
[34] G. H. Lander, *Handbook on the Physics and Chemistry of Rare Earths*, edited by K. A. Gschneidner, Jr., L. Eyring, G. H. Lander, and G. R. Choppin (Elsevier Science, Amsterdam 1993), Vol. 17, p. 635.
[35] K. Held, M. Ulmke, N. Blümer, and D. Vollhardt, Phys. Rev. B **56**, 14469 (1997) and reference therein.
[36] E. Colineau, F. Boudarot, P. Burlet, J.-P. Sanchez, and J. Larroque, Physica B **230–232**, 773 (1997).
[37] K. Kaneko, N. Metoki, N. Bernhoeft, G. H. Lander, Y. Ishii, S. Ikeda, Y. Tokiwa, Y. Haga, and Y. Ōnuki, Phys. Rev. B **68**, 214419 (2004).
[38] S. Ikeda, Y. Tokiwa, Y. Haga, E. Yamamoto, T. Okubo, M. Yamada, N. Nakamura, K. Sugiyama, K. Kindo, Y. Inada, H. Yamagami, and Y. Ōnuki, J. Phys. Soc. Jpn. **72**, 576 (2003).
[39] H. Onishi and T. Hotta, New J. Phys. **6**, 193 (2004).
[40] P. Burlet, J. Rossat-Mignod, G. H. Lander, J. C. Spirlet, J. Rebizant, and O. Vogt, Phys. Rev. B **36**, 5306 (1987).
[41] M. Wulff, O. Eriksson, B. Johansson, B. Lebech, M. S. S. Brooks, G. H. Lander, J. Rebizant, J. C. Spirlet, and P. J. Brown, Europhys. Lett. **11**, 269 (1990).
[42] A. Hiess, F. Boudarot, S. Coad, P. J. Brown, P. Burlet, G. H. Lander, M. S. S. Brooks, D. Kaczorowski, A. Czopnik, and R. Troc, Europhys. Lett. **55**, 267 (2001).
[43] M. S. S. Brooks, Physica B **345**, 93 (2004) and reference therein.
[44] Yamagami (private communication).